Experimental Evaluation of Linear Array Calibration by using 2-D Virtual Array

Hiroshi SAKAI [1], Hiroyoshi YAMADA [2], Yoshio YAMAGUCHI [2]
[1] Graduate School of Science & Technology, Niigata University
Ikarashi 2–8050, Niigata-shi, 950–2181 Japan,
sakai@wave.ie.niigata-u.ac.jp
[2] Faculty of Engineering, Niigata University
Ikarashi 2–8050, Niigata-shi, 950–2181 Japan,
{yamada,yamaguch}@ie.niigata-u.ac.jp

1. Introduction

In recent years, high-resolution Direction-of-Arrival (DOA) estimation techniques with an array antenna such as the MUSIC [1] have been applied in various fields. There are a lot of error factors when array antenna is used for the DOA estimation. DOA estimation accuracy deteriorates significantly due to the errors in actual measurements. When reference data for calibration are obtained in advance, the error factors can be estimated. For azimuth only DOA estimation, a uniform linear array is often employed. However, when elevation angle dependency for DOA estimation exists in the array, the DOA estimation performance of azimuth angle also deteriorates in general. To calibrate this error, we introduce additive virtual elements to the linear array forming a virtual rectangular array, and propose a 2-D calibration technique with the virtual array. In this report, we show the availability of the proposed 2-dimensional calibration by the virtual array, and make a comparative analysis of calibration accuracy on the conventional and the proposed calibration method, respectively, by experiment.

2. The Data Model

In this report, we employ an L-element linear array as shown in Fig.1. Assuming that K incoming waves having azimuth angle of $\theta_k (k = 1, \cdots, K)$ impinge on the array, the received data vector $\boldsymbol{x}(t)$ can be written by

$$\begin{aligned} \boldsymbol{x}(t) &= \boldsymbol{A}\boldsymbol{s}(t) + \boldsymbol{n}(t), & (1)\\ \boldsymbol{A} &= [\boldsymbol{a}(\theta_1), \cdots, \boldsymbol{a}(\theta_K)], & (2)\\ \boldsymbol{a}(\theta_k) &= [e^{-j\frac{2\pi}{\lambda}d_1 \sin\theta_k}, \cdots, e^{-j\frac{2\pi}{\lambda}d_L \sin\theta_k}]^T, & (3)\\ \boldsymbol{s}(t) &= [s_1(t), \cdots, s_K(t)]^T, & (4) \end{aligned}$$

where $\boldsymbol{a}(\theta_k)$ is the ideal mode vector (without error), $\boldsymbol{A}$ is the $L \times K$ mode matrix, $\boldsymbol{s}(t)$ is the complex amplitude vector, $\boldsymbol{n}(t)$ is the additive white Gaussian noise vector, and ^{T} denotes the transpose. In (3), elevation angle of the waves are assumed to be zero. If elevation angle is varied and the array has angle dependent error, the mode vector cannot be written by (3). To include this elevational effect, one may modify the mode vector and mode matrix of the array as,

$$\begin{aligned} \boldsymbol{a}(\theta_k, \phi_k) &= [e^{-j\frac{2\pi}{\lambda}d_1 \sin\theta_k \cos\phi_k}, \cdots, e^{-j\frac{2\pi}{\lambda}d_L \sin\theta_k \cos\phi_k}]^T, & (5)\\ \boldsymbol{A}(\boldsymbol{\theta}, \boldsymbol{\phi}) &= [\boldsymbol{a}(\theta_1, \phi_1), \cdots, \boldsymbol{a}(\theta_K, \phi_K)], & (6)\\ \boldsymbol{\phi} &= [\phi_1, \cdots, \phi_K], & (7) \end{aligned}$$

3. The Conventional Calibration Method

If we have several data set for calibration data that contain one wave of known DOA in each, the received data vector can be written by

$$\boldsymbol{x}(\theta, \phi) = \boldsymbol{G}(\theta, \phi)\boldsymbol{a}(\theta, \phi)s(t), \quad (8)$$

where $\boldsymbol{G}$ is an $L \times L$ diagonal error matrix which contains error coefficients of the antenna. In (8), we ignore the noise vector for simplicity. The error matrix $\boldsymbol{G}$ can be written by

$$\boldsymbol{G}(\theta, \phi) = \tilde{\boldsymbol{X}}(\theta, \phi)\boldsymbol{A}^{-1}(\theta, \phi), \quad (9)$$
$$\tilde{\boldsymbol{X}}(\theta, \phi) = \mathrm{diag}\{\boldsymbol{x}(\theta, \phi)\}, \quad (10)$$
$$\boldsymbol{A}(\theta, \phi) = \mathrm{diag}\{\boldsymbol{a}(\theta, \phi)\}, \quad (11)$$

If we extend the processing for all of calibration data $\boldsymbol{x}(\theta_i, \phi_j)$, $i = 1 \sim M_\theta$, $j = 1 \sim M_\phi$, where M_θ and M_ϕ are the number of calibration angles for θ and ϕ, respectively, we have $\boldsymbol{G}(\theta_i, \phi_j)$s. In addition, $\boldsymbol{G}(\theta, \phi)$ for arbitrary (θ, ϕ) can be estimated by interpolation with the nearest 4-$\boldsymbol{G}$s ($\boldsymbol{G}(\theta_i, \phi_j)$, $\boldsymbol{G}(\theta_{i+1}, \phi_j)$, $\boldsymbol{G}(\theta_i, \phi_{j+1})$ and $\boldsymbol{G}(\theta_{i+1}, \phi_{j+1})$).

4. The Proposed Calibration Method

One of the other conventional calibration techniques uses a constant calibration matrix $\boldsymbol{C}$ instead of $\boldsymbol{G}(\theta, \phi)$. If the errors have no azimuth (θ) dependency, the $L \times L$ calibration matrix $\boldsymbol{C}(\phi)$ holds,

$$\boldsymbol{X}(\boldsymbol{\theta}, \phi) = \boldsymbol{C}(\phi)\boldsymbol{A}(\boldsymbol{\theta}, \phi), \quad (12)$$

where $\boldsymbol{X}(\boldsymbol{\theta}, \phi)$ is the calibration data matrix whose column includes diverse azimuth angle data of the same ϕ, and $\boldsymbol{A}(\boldsymbol{\theta}, \phi)$ is the ideal mode matrix corresponding to the waves. Azimuth dependent error can be compensated effectively by using the $L \times L$ matrix $\boldsymbol{C}(\phi)$. However, we cannot remove elevational error by this model. Therefore, to solve the problem, we propose to introduce additive virtual elements to the linear array so as to form a virtual rectangle array. If we place L_x-elements and L_z-elements in the direction of the x-axis and z-axis, respectively, as shown in Fig.2, the $L_z \times L_x$ rectangular array is obtained. Using this virtual array arrangement the received data vector can be written by

$$\boldsymbol{x}(\theta, \phi) = \boldsymbol{C}_{\mathrm{ex}}\boldsymbol{a}_{\mathrm{ex}}(\theta, \phi), \quad (13)$$
$$\boldsymbol{a}_{\mathrm{ex}}(\theta_i, \phi_i) = \boldsymbol{a}_x(\theta_i, \phi_i) \otimes \boldsymbol{a}_z(\phi_i), \quad (14)$$
$$\boldsymbol{a}_x(\theta_i, \phi_i) = [e^{-j\frac{2\pi}{\lambda}x_1 \sin\theta_i \cos\phi_i}, \cdots, e^{-j\frac{2\pi}{\lambda}x_{L_x} \sin\theta_i \cos\phi_i}], \quad (15)$$
$$\boldsymbol{a}_z(\phi_i) = [e^{j\frac{2\pi}{\lambda}z_1 \sin\phi_i}, \cdots, e^{j\frac{2\pi}{\lambda}z_{L_z} \sin\phi_i}], \quad (16)$$

where $\boldsymbol{a}_{\mathrm{ex}}$ is the mode vector of the virtual rectangle array, and $\otimes$ denotes the Kronecker product. Derivation of the extended calibration matrix $\boldsymbol{C}_{\mathrm{ex}}$ can be done as follows. The calibration matrix $\boldsymbol{C}(\phi_i)$ in (12) has the relation:

$$\begin{aligned}\boldsymbol{C}(\phi_i) &= \boldsymbol{C}_{\mathrm{ex}}\boldsymbol{A}_{\mathrm{ex}}(\boldsymbol{\theta}, \phi_i)\boldsymbol{A}(\boldsymbol{\theta}, \phi_i)^H \left(\boldsymbol{A}(\boldsymbol{\theta}, \phi_i)\boldsymbol{A}(\boldsymbol{\theta}, \phi_i)^H\right)^{-1} \\ &= \boldsymbol{C}_{\mathrm{ex}}\boldsymbol{P}_i, \end{aligned} \quad (17)$$
$$\boldsymbol{A}_{\mathrm{ex}}(\boldsymbol{\theta}, \phi_i) = [\boldsymbol{a}_{\mathrm{ex}}(\theta_1, \phi_i), \cdots, \boldsymbol{a}_{\mathrm{ex}}(\theta_K, \phi_i)], \quad (18)$$

where ^{H} denotes the complex conjugate transpose. If we have N different calibration matrix $\boldsymbol{C}(\phi_i)$, $i = 1, 2, \cdots, N$, the next equation can be obtained:

$$[\boldsymbol{C}(\phi_1) \cdots \boldsymbol{C}(\phi_N)] = \boldsymbol{C}_{\mathrm{ex}}\,[\boldsymbol{P}_1 \cdots \boldsymbol{P}_N]\,. \quad (19)$$

When we define $\boldsymbol{C}_{\mathrm{all}}$ and $\boldsymbol{P}_{\mathrm{all}}$ by the left-side matrices of $\boldsymbol{C}(\phi_i)$s and right-side matrices of $\boldsymbol{P}_i$s, respectively, the extended calibration matrix $\boldsymbol{C}_{\mathrm{ex}}$ can be derived by

$$\boldsymbol{C}_{\mathrm{ex}} = \boldsymbol{C}_{\mathrm{all}}\boldsymbol{P}_{\mathrm{all}}^H(\boldsymbol{P}_{\mathrm{all}}\boldsymbol{P}_{\mathrm{all}}^H)^{-1}. \quad (20)$$

See [2] for more details.

Table 1: Experimental Parameters

Element antenna	Quarter-wavelength monopole
Number of real array elements	4
Number of virtual rectangle array elements	12 (3 × 4)
Frequency	2.45 [GHz]
Element separation	0.5 wavelength
Wire radius of each element	0.5 [mm]
Impedance of each element	50 [Ω]
DOA of reference waves (Azimuth angle)	−60° ∼ +60° 9 waves with every 15° separation
DOA of reference waves (Elevation angle)	0° ∼ +24° 5 waves with every 6° separation

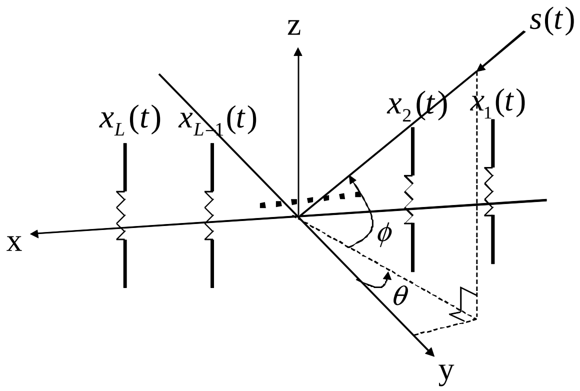

Figure 1: Uniform Linear Array

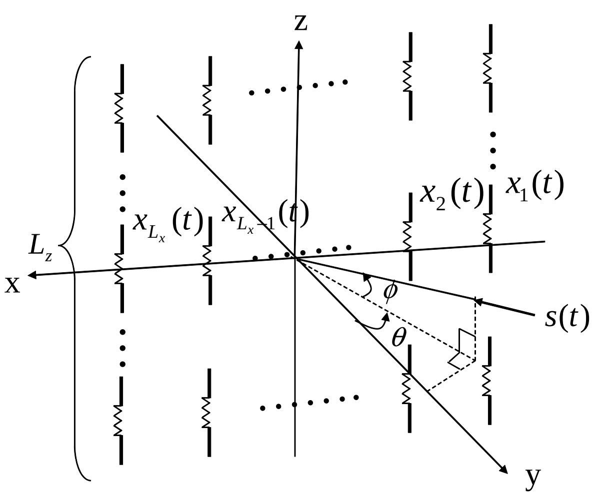

Figure 2: Uniform Rectangular Array

5. Experimental Results

In this section, we show experimental results to evaluate calibration performance of the conventional and proposed calibration methods. Experimental parameters used in this experiment are listed in Table.1. We employ a 3×4 virtual rectangle array whose z-aligned virtual elements are assumed to be located on $\pm 0.125\lambda$ with respect to the center of the adjacent real array element.

In the DOA estimation, two uncorrelated waves are employed. DOA of the first and the second waves are $(\theta_1, \phi_1) = (10°, 0°)$ and $(\theta_2, \phi_2) = (20°, 15°)$, respectively. Figure 3 shows the azimuth DOA estimation results by the MUSIC algorithm. In these estimations, calibration waves for $\phi = 0°$ are used, therefore elevational error is not calibrated. The dashed and solid line show the results calibrated by the interpolated mode vectors (as shown in Sec.3 with $\phi = 0$) and by the $L \times L$ calibration matrix $\boldsymbol{C}(\phi = 0)$, respectively. On the other hand, Figure 4 shows the azimuth DOA estimation results of the MUSIC algorithm by the conventional (Sec.3) and proposed (Sec.4) method. In this figure, peak value at each ϕ is plotted as the function of azimuth angle (θ). The estimated angles by the conventional and the proposed method are $(\theta_1, \theta_2) = (10.4°, 20.8°)$ and $(\theta_1, \theta_2) = (10.3°, 19.6°)$, respectively, and the accuracy of azimuth angle estimation is improved. Figures 5(a) and (b) show the 2-D MUSIC spectrum by the conventional and the proposed method, respectively. The MUSIC spectrum with the conventional method has several spurious peaks at non-DOA angles, then precise DOA estimation cannot be realized. On the other hand, the MUSIC spectrum with the proposed method has two peaks clearly, and precise DOA estimation can be realized.

6. Conclusions

In this report, we proposed a 2-D calibration by using the virtual array, and show its availability by the experiment. Peak characteristic of the MUSIC spectrum can be improved by the proposed 2-D extended calibration. This means that DOA estimation and detection performance is enhanced by the proposed calibration technique.

Acknowledgement

This work was supported by KAKENHI (2056349) and the Grant-in-Aid for engineering research of TELEC.

References

[1] R. O. Schmidt, "Multiple emitter location and signal parameter estimation," IEEE Trans. Antennas Propag., vol.AP-34, no.3, pp.276–280, Mar. 1986.

[2] T.Naito, H.Yamada, Y.Yamaguchi, "On calibration of elevation angle dependancy for DOA estimation with linear array using virtual array," IEICE Technical Report, vol.A·P2007-130, pp.45-50, Jan. 2008 *(in Japanese)*.

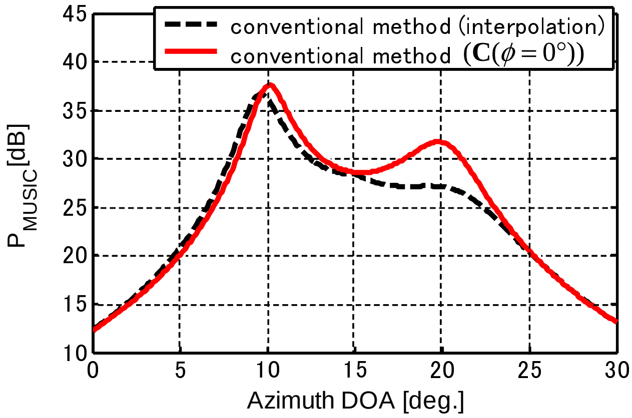

Figure 3: Azimuth DOA estimation results by the conventional calibration techniques (1-D search)

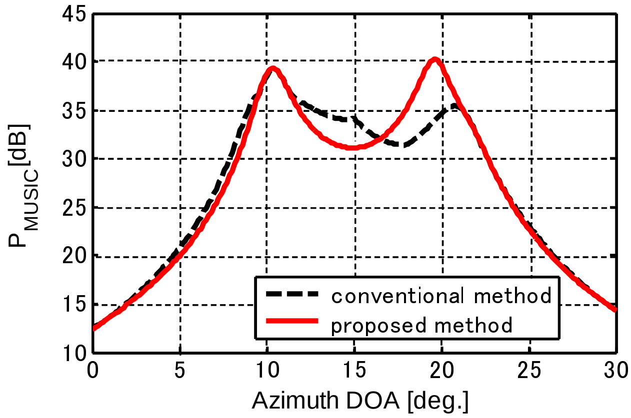

Figure 4: Maximum value of P_{MUSIC} at each azimuth angle (2-D search)

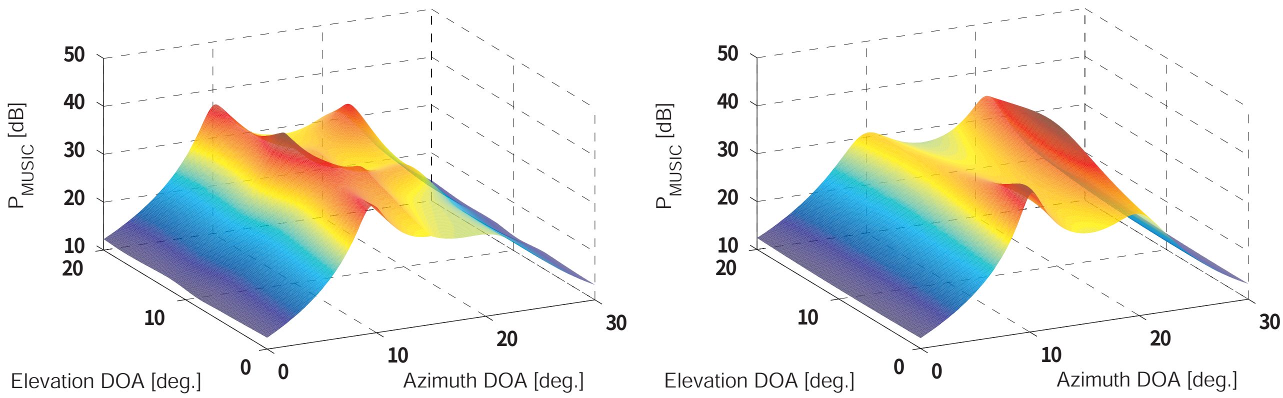

(a) Conventional method (b) Proposed method

Figure 5: The 2-D MUSIC spectrum